Journal of Alloys and Compounds 508 (2010) 110–114

Contents lists available at ScienceDirect

Journal of Alloys and Compounds

journal homepage: www.elsevier.com/locate/jallcom

The effect of tin addition on the microstructure and mechanical properties of squeeze cast AM60 alloy

Hüseyin Sevik, Sehzat Açıkgöz, S. Can Kurnaz*

Sakarya University, Faculty of Engineering, Department of Metallurgical and Materials Engineering, Adapazarı 54187, Turkey

ARTICLE INFO

Article history:
Received 3 December 2009
Received in revised form 26 July 2010
Accepted 28 July 2010
Available online 5 August 2010

Keywords:
AM60 alloy
Squeeze-casting process
Microstructure
Mechanical properties

ABSTRACT

In this study, the effect of tin addition (0, 0.5, 1, 2 and 4 wt% Sn) on the microstructure and mechanical properties of a magnesium-based alloy (AM60) were investigated. The alloys were produced under a controlled atmosphere by a squeeze-casting process. The results indicated that Sn addition effectively decreased the dimension of eutectic phase region on the grain boundary. The hardness value of AM60 alloy increased with the increment of alloying element ingredients. The tensile testing results indicated that the greatest ultimate tensile strength (UTS) was exhibited by AM60–4 wt% Sn as 212 MPa. The impact strength of AM60 alloy was remarkably increased by 0.5 wt% Sn addition from 16 J in initial state to 24 J. Having added to this critical weight percentage tin ratio, the impact strength starts to decrease with increasing Sn addition.

1. Introduction

Magnesium alloys have vital importance due to weight reduction in the vehicles because of their lower density and high strength-to-weight ratio. The utilization of magnesium and its alloys in the automotive industry has therefore significantly increased in past few years [1–3]. However, only a few magnesium alloys especially produced by pressure die-casting are used since it has lower mechanical properties and corrosion resistance than that of aluminum alloys [4,5]. In general, magnesium alloys are based on Mg–Al systems and it is well known, Al containing Mg alloys include the β-$Mg_{17}Al_{12}$ compound that detrimentally influences the mechanical properties [5–7]. Therefore, the third alloying element such as stronsium (Sr), calcium (Ca), and tin (Sn) are added to these alloys in order to improve the mechanical properties [3,8–11]. In view of the Mg–Sn binary phase diagram, the solubility of Sn in the α-Mg solid solution drops sharply from 14.85 wt% at the eutectic transformation temperature of 561 °C to 0.45 wt% at 200 °C and these alloy systems have thermal stable Mg_2Sn intermetallics [11]. As a result, it was observed that addition of Sn can improve the mechanical properties of Mg–Al alloys and their usage is more economical than that of other magnesium alloys. However, very little studies on the mechanical properties of these alloys have been accomplished and not been clearly identified yet [12–15]. Hence, the present study focuses on the microstructure and mechanical properties of AM60 alloy with the addition of Sn.

2. Experimental details

The alloys, with compositions listed in Table 1, were prepared in a steel crucible with an electric resistance furnace protected by CO_2–1% SF_6 from commercially pure magnesium, aluminum and tin. Manganese was added in Al–10Mn form as a master alloy. The casting parameters were as follows: the melt was held at 720 °C casting temperature for 20 min, and stirred to ensure the homogeneity in a mold at 150 °C and with 100 MPa filling pressure.

Metallographic samples were cut firstly on a wire erosion machine. Grinding was performed using silicon carbide (SiC) grinding papers up to 1200 grit. Prior to polishing, the samples were rinsed with ethanol, and then polishing was performed with a 0.05 μm alumina solution. The specimens for optical microscopy (OM) were chemically etched in acetic picric (5 ml acetic acid, 6 g picric acid, 10 ml distilled water, 100 ml ethanol) to show grain boundaries and nital (4 ml nitric acid, 96 ml ethanol) for revealing structure. In addition, the distribution of alloying elements in the structure was verified by using a scanning electron microscopy (SEM) instrument (JEOL 6060LV) with an energy-dispersive spectrometer (EDS). X-ray diffraction (XRD) analysis was also carried out to identify the phases present in the experimental alloys using a Rigaku D-Max 1000 X-ray diffractometer with Cu Kα radiation.

Brinell hardness tests of the alloys were carried out on ground and polished samples with a ball diameter of 2.5 mm and an applied load of 31.25 kg. At least 10 impressions were made to determine the mean value of the hardness at different locations to circumvent the effect of any alloying element segregation. Tensile tests were performed using an Instron 3367 universal testing machine with a strain rate of 0.2 mm/s at room temperature. Each test was repeated for ten times, and the average values were accepted as the experimental result. Un-notched impact test samples were cut on a wire erosion machine and test specimens measured 55 mm × 10 mm × 10 mm and then polished. The testing was carried out using a Charpy impact test machine at room temperature and at least three runs were performed.

* Corresponding author. Tel.: +90 2642955789; fax: +90 2642955600.
E-mail address: ckurnaz@sakarya.edu.tr (S. Can Kurnaz).

0925-8388/$ – see front matter © 2010 Elsevier B.V. All rights reserved.
doi:10.1016/j.jallcom.2010.07.185

Table 1
The chemical composition of the investigated alloys (mass fraction, %).

Alloy	Al	Mn	Sn	Si	Fe	Mg
AM60	5.93	0.18	–	<0.02	0.013	Bal.
AM60–0.5Sn	5.92	0.16	0.47	<0.02	0.015	Bal.
AM60–1Sn	5.95	0.15	0.94	<0.02	0.021	Bal.
AM60–2Sn	5.90	0.22	1.83	<0.02	0.022	Bal.
AM60–4Sn	5.97	0.17	3.94	<0.02	0.019	Bal.

3. Results and discussion

3.1. Microstructure and characterization

Fig. 1 shows the influence of different amounts of Sn addition into AM60 alloy on the grain size. It obviously shows that the grain size of AM60 alloy decreases with increasing quantity of Sn addition. The grain size of the alloy decreases from 107 to 55 μm when the amount of Sn added increases from 0 to 4 wt%, respectively.

Figs. 2 and 3 show OM and EDS analyses of the AM60 alloy with different amounts of Sn additions, respectively. Microstructure of the AM60 alloy mainly consists of primary α-Mg dendrite grains with eutectic phases (Al-riched α-Mg + β-$Mg_{17}Al_{12}$) surrounding their boundaries (Fig. 2(a)). According to the ratio of Al to Mn, it could be deduced that the first spot in Fig. 3(a) was AlMn phase and the second spot could be decided as β-$Mg_{17}Al_{12}$ phase. The microstructures of AM60 alloy with 0.5 and 4 wt% Sn are shown in Fig. 2(b) and (c). When these figures were compared with Fig. 2(a), it was noticed that the microstructure of the alloys indicate some changes with increasing Sn content. While adding Sn element, it can be clearly seen that the dimension of eutectic phase on the grain boundary decreases. It means that Sn element assists to refine the eutectic phase on the grain boundary. Fig. 3(b) shows the EDS analyses of AM60 + 0.5Sn. In Fig. 3(b) the spots were indicated that some Sn was solved both in the primary α-Mg grains and $Mg_{17}Al_{12}$ phase. Furthermore, adding 0.5 wt% Sn to AM60 alloy modified by $Mg_{17}Al_{12}$ with decreasing size of the particles (Fig. 3(b), spots 2 and 3). However, it can be seen in Fig. 3(c) that the Mg_2Sn with sharp corner was found in the AM60–4Sn alloy and which were distributed on β-$Mg_{17}Al_{12}$. The presence of these phases was confirmed by XRD (Fig. 4). It can be seen in Fig. 4 that β-$Mg_{17}Al_{12}$ and AlMn, which were consistent with the findings of SEM and EDS, were detected in all specimens and with adding Sn element, while increasing the amount of Mg_2Sn phase the amount of β-phase was greatly reduced.

The hardness, ultimate tensile strength, elongation and impact strength values of these alloys were listed in Table 2. As can be seen from Table 2, the hardness value of AM60 alloy increases with increasing alloying element concentration. Among the Sn-containing AM60 alloys, the AM60 alloy with 2 wt% Sn exhibits the best hardness increment as 28% (from 45HRB–58HRB) higher than those of the AM60 alloy without adding Sn. This is probably

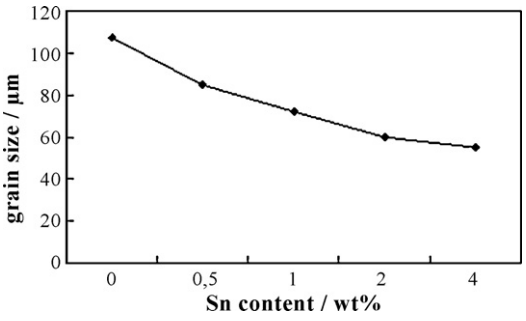

Fig. 1. The effect of Sn on grain size of AM60 alloy.

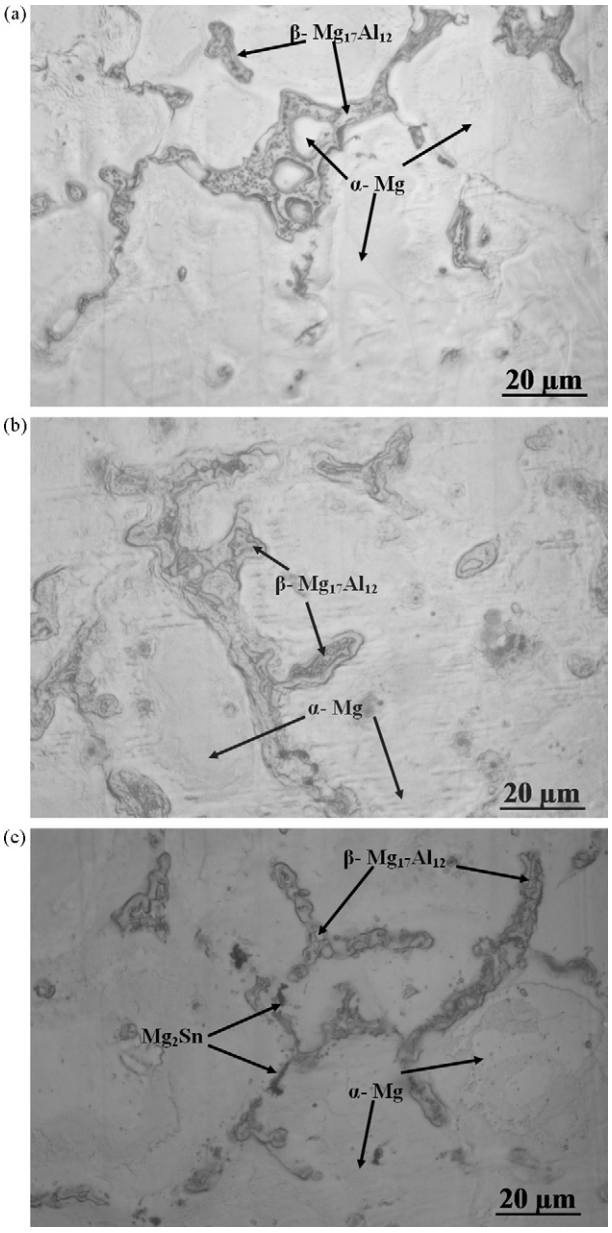

Fig. 2. Optical microstructures of: (a) AM60, (b) AM60–0.5Sn, (c) AM60–4Sn.

the result of solid solution hardening due to the solubility of Sn in the primary α-Mg. Furthermore, with increasing alloying element, Mg_2Sn intermetallic phase occurred at the grain boundaries which can help to improve the hardness of it.

The results of tensile tests reveal that rise of Sn concentration causes an increment in tensile strength, while decreasing the elongation of the alloy. The ultimate tensile strength of AM60 alloy was improved by 35% (from 156 to 212 MPa) due to the addition of 4 wt% Sn. Generally, the mechanical properties of the alloys can improve via solid solution strengthening or/and precipitation strengthening. Besides the size, shape, quantity and distribution of secondary phases can influence the mechanical properties of the alloy [13,16–18]. In this study, the improvement of the tensile strength of the AM60 alloy mainly comes from the solid solution strengthening, as mentioned before fine microstructure due to the Sn and existing Mg_2Sn intermetallic. It is believed that the above effects can help to hinder deformation. Furthermore, detrimental effect of the β-$Mg_{17}Al_{12}$ phase on the tensile strength reduced with increasing Sn element due to amount of the β-phase decreased. On

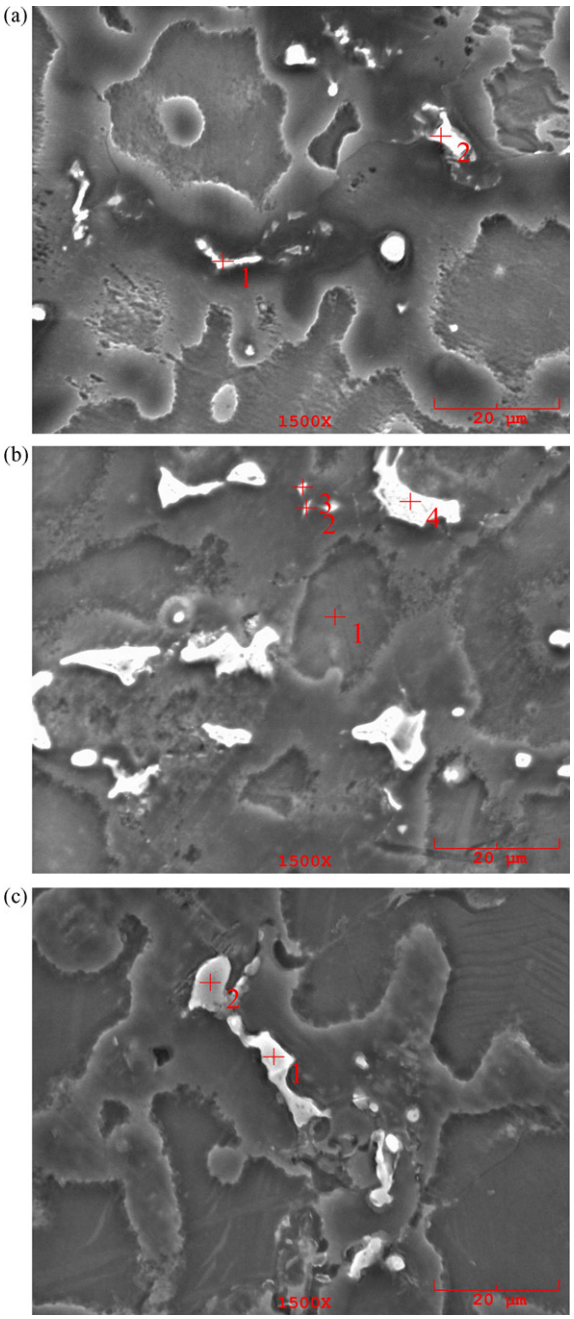

Fig. 3. EDS patterns of (a) squeeze cast AM60, (b) AM60–0.5Sn, (c) AM60–4Sn alloy (all analyses in the table is at.%).

(a) Spot no.	Chemical composition (at.%)					Atomic ratio	
	Al	Mn	Sn	Si	Mg	Mg/Al	Al/Mn
1	32.88	12.46	–	1.22	53.44	1.62	2.63
2	31.88	0.00	0.00	0.00	68.12	2.13	–

(b) Spot no.	Chemical composition (at.%)					Atomic ratio		
	Al	Mn	Sn	Si	Mg	Mg/Al	Al/Mn	Mg/Sn
1	3.57	0.00	0.42	0.00	96.01	26.89	–	–
2	32.89	1.60	1.22	1.40	62.89	1.91	20.55	51.54
3	16.58	0.21	0.70	0.00	82.51	4.97	–	–
4	39.36	0.00	0.24	0.00	60.40	1.53	–	–

(c) Spot no.	Chemical composition (at.%)					Atomic ratio	
	Al	Mn	Sn	Si	Mg	Mg/Al	Mg/Sn
1	2.17	0.00	23.82	12.71	57.30	26.4	2.4
2	35.42	0.00	0.00	0.00	64.58	1.82	–

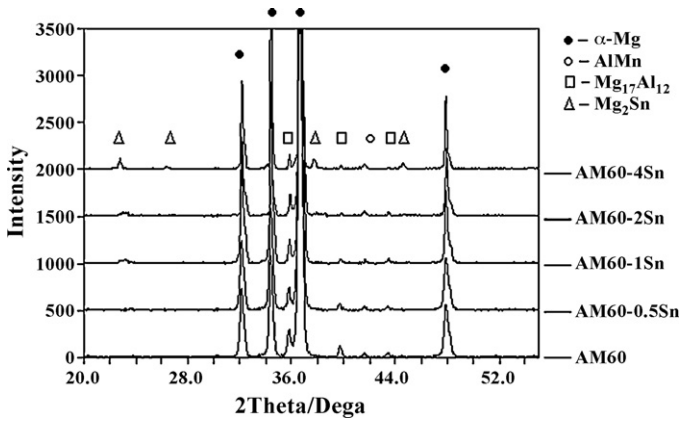

Fig. 4. The XRD spectrum of AM60 alloys with different Sn contents.

the other hand, the elongation of AM60 alloy is decreased due to the amount of Mg_2Sn phase in the AM60 alloy increases with increasing Sn concentration. Because, Mg_2Sn phase in this study have polygonal and sharp corner morphology (Fig. 3(c)). Hence, it behaves like a notch and affects the elongation value negatively. Furthermore, as was shown before Mg_2Sn intermetallic formed on the $Mg_{17}Al_{12}$. It is thought that the interface effect of the two compounds can play an important role for decreasing the strain.

The impact strength value of AM60 alloy was found 16 J. The result was in accordance with literature. Similar results were reported by Schwam et al. [4]. As can be seen at Table 2, the impact strength of AM60 alloy was remarkably increased by 0.5 wt% Sn-containing alloy. The impact strength of AM60 alloy was improved by 50% (from 16 to 24 J) due to the addition of 0.5 wt% Sn. Then the impact strength decreased with increasing Sn but this value is still higher than AM60 alloy's value (16 J). The decrease in the impact strength with increasing Sn content was attributed the sharp corner shape Mg_2Sn, increase of the amount of Mg_2Sn and the formation of Mg_2Sn compound on $Mg_{17}Al_{12}$. The main parameters affecting the impact strength are solid solution hardening due to the solubility of the alloying element and fine microstructure.

$Mg_{17}Al_{12}$ has a body-centered cubic (bcc) structure, and the magnesium matrix has a hexagonal closed packed (hcp) crystal structure. Hence, the $Mg_{17}Al_{12}$ phase is incompatible with the magnesium matrix, which results in an incoherent and fragile $Mg/Mg_{17}Al_{12}$ interface [19]. Consequently, microcracks tend to initiate at the $Mg/Mg_{17}Al_{12}$ interface and even in the $Mg_{17}Al_{12}$ phase. In the examination of Fig. 5(a)–(c), we can see that the incompatible interface length in AM60 alloy is bigger than the others. As can be seen in Fig. 5(a), the fracture in the as-cast AM60 alloy took place along the continuous network structure of the $Mg_{17}Al_{12}$ phase; however, the fractures in the Sn-containing alloys occurred throughout the Mg matrix and $Mg/Mg_{17}Al_{12}$ interface as well. This situation was contributed to restricting crack propagation.

Table 2
Hardness, ultimate tensile, elongation and impact strength of the tested materials.

	Hardness (HBN)	UTS (MPa)	ε (%)	Impact strength (J)
AM60	45 ± 2	156 ± 6	10.7 ± 0.4	16 ± 1
AM60–0.5Sn	50 ± 1	182 ± 4	10.0 ± 0.8	24 ± 2
AM60–1Sn	54 ± 0	190 ± 4	9.7 ± 0.3	21 ± 2
AM60–2Sn	58 ± 1	210 ± 5	9.1 ± 1.1	18 ± 1
AM60–4Sn	58 ± 2	212 ± 4	8.1 ± 0.7	17 ± 2

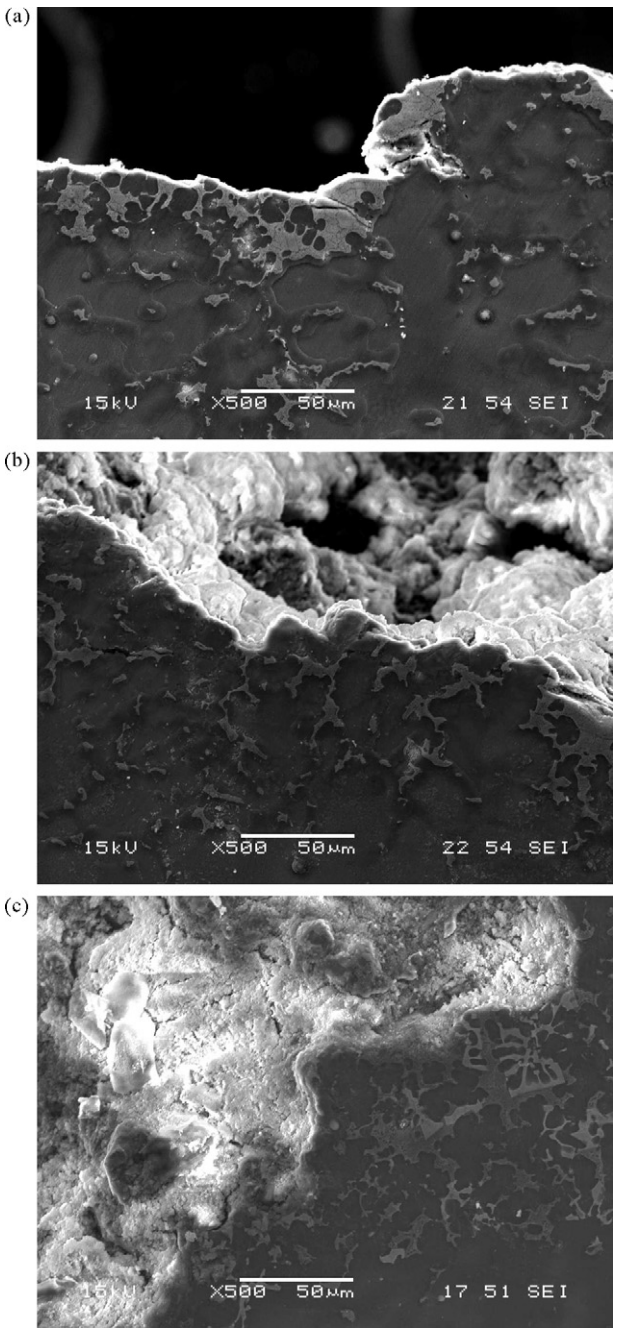

Fig. 5. SEM result for the cross-section of the specimen failed in tensile test: (a) AM60, (b) AM60–0.5Sn and (c) AM60–4Sn alloy.

4. Conclusions

In this present study, influence of addition of Sn on the microstructure and mechanical properties of squeeze cast AM60 alloy have been investigated. The following results were obtained:

(1) Metallographic studies showed that the addition of Sn changed the microstructure of AM60 alloy. Sn element assists to refine the eutectic phase on the grain boundary. By addition of 0.5 wt% Sn to AM60 alloy, some Sn was solved both in the primary α-Mg grains and $Mg_{17}Al_{12}$ phase. Furthermore, adding 0.5 wt% Sn to AM60 alloy modified $Mg_{17}Al_{12}$ with decreasing the size of the particles. Having increased alloying element, new polyg-

onal Mg_2Sn intermetallic phase was occurred at the grain boundaries.

(2) The hardness value of AM60 alloy increased with increasing alloying element concentration. Among the Sn-containing AM60 alloys, the highest hardness value was obtained in AM60 alloy with 2 wt% Sn content as 58 HB.

(3) This increase in Sn concentration causes a rise in tensile strength, while decreasing the elongation of the alloy. The best ultimate tensile strength value was obtained by the AM60 alloy with 4 wt% Sn as 212 MPa.

(4) The impact energy of AM60 alloy was remarkably increased from 16 to 24 J by 0.5 wt% Sn-containing alloy, and then the impact energy absorbing capacity was decreased with increasing Sn.

References

[1] A.A. Luo, Journal of Materials (February) (2002) 42–48.
[2] E. Aghion, B. Bronfin, H. Friedrich, Z. Rubinovich, in: H.A. Luo (Ed.), Magnesium Technology, TMS, USA, 2004, pp. 167–172.
[3] Y.V.R.K. Prasad, K.P. Rao, N. Hort, K.U. Kainer, Materials Science and Engineering A 502 (2009) 25–31.
[4] D. Schwam, J.F. Wallace, Y. Zhu, DOE-FC07-98ID13611, U.S. Department of Energy Assistant Secretary for Energy Efficiency and Renewable Energy, Washington, DC, June 2000.
[5] T.A. Leil, N. Hort, W. Dietzel, C. Blawert, Y. Huang, K.U. Kainer, K.P. Rao, Transactions of Nonferrous Metals Society of China 19 (2009) 40–44.
[6] S. Kleiner, O. Beffort, A. Wahlen, P.J. Uggowitzer, Journal of Light Metals 2 (2002) 277–280.
[7] G Song, Corrosion Science 51 (2009) 2063–2070.
[8] H. Liu, Y. Chen, H. Zhao, S. Wei, W. Gao, Journal of Alloys and Compounds 504 (2010) 345–350.
[9] S. Li, B. Tang, D. Zeng, Journal of Alloys and Compounds 437 (2007) 317–332.
[10] S. Cohen, G.R. Goren-Mugistein, S. Avraham, G. Dehm, M. Bamberger, in: H.A. Luo (Ed.), Magnesium Technology, TMS, USA, 2004, pp. 301–305.
[11] N. Hort, Y. Huang, K.U. Kainer, Advanced Engineering Materials 8 (2006) 235–240.
[12] P. Bakke, K. Pettersen, D. Albright, in: H.A. Luo (Ed.), Magnesium Technology, TMS, USA, 2004, pp. 289–296.
[13] C. Jihua, C. Zhenhua, Y. Hongge, Z. Fuquan, Journal of Alloys and Compounds 467 (2009) l1–l7.
[14] A.L. Bowles, C. Blawert, N. Hort, K.U. Kainer, in: H.A. Luo (Ed.), Magnesium Technology, TMS, USA, 2004, pp. 307–310.
[15] Z. Min, Z. Wen-zheng, Z. Guo-zhen, Y. Kun, Transactions of Nonferrous Metals Society of China 17 (2007) 1428–1432.
[16] J. Zhang, D. Zhang, Z. Tian, J. Wang, K. Liu, H. Lu, D. Tang, J. Meng, Materials Science and Engineering A 489 (2008) 113–119.
[17] D.K. Xu, L. Liu, Y.B. Xu, E.H. Han, Journal of Alloys and Compounds 426 (2006) 155–161.
[18] B.J. Coultes, J.T. Wood, G. Wang, R. Berkmortel, in: H.I. Kaplan (Ed.), Magnesium Technology, TMS, USA, 2003, pp. 45–50.
[19] Y.Z. Lu, Q.D. Wang, W.J. Ding, X.Q. Zeng, Y.P. Zhu, Materials Letters 44 (2000) 265–268.